Cooling and freshening of the West Spitsbergen Current by shelf-origin cold core lenses

Zoé Koenig, Amelie Meyer, Christine Provost, Nathalie Sennéchael, Arild Sundfjord, Laurent Béguery, Marylou Athanase, Jean-Claude Gascard

AGU100 ADVANCING EARTH AND SPACE SCIENCE

JGR

Journal of Geophysical Research: Oceans

RESEARCH ARTICLE

10.1029/2018JC014463

Key Points:

- A SeaExplorer glider made six sections across the West Spitsbergen Current (WSC) at 78.5-79 degrees north in the Arctic
- Cold and fresh small-core lenses originating from the Svalbard shelf, observed in the core of the WSC contribute to the cooling of the WSC
- Shelf waters flow to bottom of the slope through diapycnal displacement and detached in lenses through isopycnal displacement

Correspondence to:
Z. Koenig,
zklod@locean-ipsl.upmc.fr

Citation:
Koenig, Z., Meyer, A., Provost, C., Sennéchael, N., Sundfjord, A., Beguery, L., et al. (2018). Cooling and freshening of the West Spitsbergen Current by shelf-origin cold core lenses. *Journal of Geophysical Research: Oceans*, *123*, 8299–8312. https://doi.org/10.1029/2018JC014463

Received 10 AUG 2018
Accepted 23 OCT 2018
Accepted article online 1 NOV 2018
Published online 19 NOV 2018

Cooling and Freshening of the West Spitsbergen Current by Shelf-Origin Cold Core Lenses

Zoé Koenig[1], Amelie Meyer[2,3], Christine Provost[1], Nathalie Sennéchael[1], Arild Sundfjord[3], Laurent Beguery[4], Marylou Athanase[1], and Jean-Claude Gascard[1]

[1]Laboratoire LOCEAN-IPSL, Sorbonne Universites (UPMC, Univ. Paris 6)-CNRS-IRD-MNHN, Paris, France, [2]ARC Centre of Excellence for Climate Extremes and Institute for Marine and Antarctic Studies, University of Tasmania, Hobart, Tasmania, Australia, [3]Norwegian Polar Institute, Fram Centre, Tromsø, Norway, [4]Alseamar, Rousset, France

Abstract The West Spitsbergen Current (WSC) cools and freshens as it flows northward along the western Svalbard shelf. The cooling takes place at the ocean surface through interaction with the atmosphere and also in subsurface. We present observations with high horizontal resolution (around 2 km) from a SeaExplorer glider deployed in July 2017 for 14 days in the WSC offshore Kongsfjorden around 79°N. They document small lenses (less than 10-km diameter) of cold (less than 3.8 °C) and fresh (less than 35.2 g/kg) waters in the core of the WSC, coming from the shelf and contributing to its cooling and freshening. Data show that water from the shelf cascades to the bottom of the slope and then detaches on the offshore side of the WSC core where it is baroclinically unstable. The presence of these lenses from the shelf can be related to the wind regime. Strong southerly winds cause upwelling of the warm Atlantic Water onto the shelf in winter. Weak and/or northerly winds allow modified Atlantic Water formed by mixing with cold waters on the shelf to cascade down the slope, leading to lenses of colder and fresher water protruding into the WSC. If lenses are common in the WSC, they could be contributing significantly to its cooling and freshening especially in summer when the influence of the atmosphere on the cooling of the WSC is less important.

Plain Language Summary The West Spitsbergen Current (WSC), which flows northward along the western Svalbard slope, carrying warm, high-salinity Atlantic Water (AW), is a main source of heat and salt to the Arctic Ocean. It cools and freshens as it flows northward. We present observations from a SeaExplorer glider deployed in July 2017 for 14 days in the WSC around 79°N. They document small lenses (less than 10 km) of cold and fresh waters from the shelf in the core of the WSC (about 250-m depth). Water from the Svalbard shelf cascades to the bottom of the slope. Cold and fresh lenses detached from the bottom of the slope. The presence of these lenses from the shelf is related with the wind regime. Strong southerly winds cause upwelling of the warm AW onto the shelf in winter. Weak and/or northerly winds allow modified AW on the shelf to cascade down the slope, leading to lenses of colder and fresher water protruding into the WSC. If lenses were common, they could be contributing significantly to the cooling and freshening of the WSC.

1. Introduction

The West Spitsbergen Current (WSC, Figure 1), which flows northward along the western Svalbard slope, carrying warm, high-salinity Atlantic Water (AW), is the main source of heat and salt to the Arctic Ocean. The WSC cools and freshens rapidly (about 0.31 °C per 100 km, Saloranta & Haugan, 2004) as it flows along the western slope of Svalbard. Saloranta and Haugan (2004) estimated that the WSC loses between 1,000 W/m^2 in winter and 300 W/m^2 in summer in the 100- to 500-m depth layer. The sources of this cooling are limited to the surrounding atmosphere, sea ice, and waters. Several studies focus on the possible origin of this cooling. Boyd and D'Asaro (1994) showed that heat loss to the atmosphere and sea ice cools the surface and part of the core of the WSC at depth. However, the rate of cooling of the WSC is too large to be explained only by cooling from the sea ice and the atmosphere, especially in summer when the atmosphere plays a less important role in the cooling of the WSC. Indeed in summer the WSC is partly capped by a fresh and cold layer that insulates the AW core from the atmosphere, and the atmosphere is often not colder than the ocean west of Svalbard, resulting in weaker heat fluxes. Other processes not related to the atmosphere have been suggested to explain the cooling of the WSC. Boyd and D'Asaro (1994) suggested that the WSC is

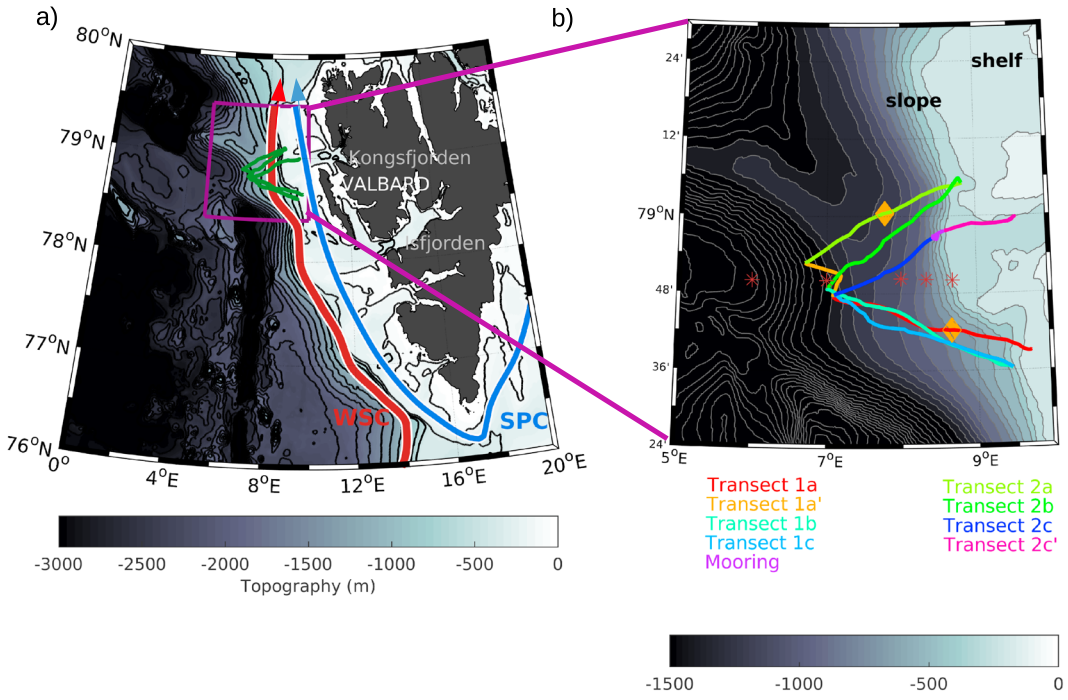

Figure 1. (a) Bathymetry from International Bathymetric Chart of the Arctic Ocean (https://www.ngdc.noaa.gov/mgg/bathymetry/arctic/ arctic.html) along the west continental slope of Svalbard. Green lines are the SeaExplorer glider trajectory in July 2017. Black lines are bathymetry. (b) Zoom on the glider trajectory (purple box). Each color corresponds to a transect. Moorings at 78.5°N from the Alfred Wegener Institute (AWI) (Beszczynska-Möller et al., 2015) are located with orange stars (F1 to F5). The yellow diamonds indicate the lens locations. SPC = Spitsbergen Polar Current; WSC = West Spitsbergen Current.

also cooled via isopycnal diffusion by mesoscale eddies that renew the surface waters and exchanges with waters west of the WSC. Since the WSC not only cools but also freshens, Saloranta and Haugan (2004) suggested exchanges with shelf waters through diapycnal mixing as the hypothesis of a pure isopycnal offshore mixing is not sufficient. Nilsen et al. (2006) investigated the high frequencies in the inshore current meter data from the mooring array at 78.83°N (Beszczynska-Möller et al., 2015). They suggested that the large eddy field in the WSC is partly generated by instabilities and that topographically trapped Rossby waves can diffuse heat along the steeply sloping isopycnal surfaces, either offshore or onshore hence cooling the core of the WSC.

We investigate the potential of the onshore waters on the shelf to participate in the cooling of the core of the WSC. The shelf waters (cold and fresh waters from the Svalbard coast and fjords joining the Spitsbergen Polar Current flowing northward from the Barents Sea, Figure 1a) and slope waters (warm and salty waters from the WSC) are separated by the Polar Front. The front is described by a density gradient at the surface and with only a temperature and salinity gradients at depth (Saloranta & Svendsen, 2001).

The shelf is a region of exchanges and mixing between the AW and the cold and fresh waters (Saloranta & Svendsen, 2001; Walczowski, 2013). The influence of the WSC on the shelf current is quite well documented. Patches of warm AW from the WSC are found on the shelf (Nilsen et al., 2016). The upwelling of AW on the shelf is substantially wind driven (Goszczko et al., 2018) with Ekman transport oriented toward the shelf in the presence of southerly winds. Warm AW is found on the shelf in winter when cyclones and storms are frequent (Cottier et al., 2007). Nilsen et al. (2016) documented the existence of a shelf current composed of slightly modified AW due to mixing of AW with fjord waters—the Spitsbergen Trough Current—which also results from persistent wind forcing.

But how does the shelf water influence the WSC and participate in the cooling of the core of the WSC? Some numerical studies have highlighted the important role of eddy overturning in the mixing at the Polar front (Tverberg & Nøst, 2009), while others have highlighted the importance of the wind pushing waters from the shelf to downwell along the slope and hence into the WSC (Goszczko et al., 2018). However, no mesoscale features/eddies of shelf origin have yet been documented through observations

Table 1
Time (UTC) and Locations of Transects Shown in Figure 1

	Start time	End time	Start position	End position
Transect 1a	24/07/2017 21h42	26/07/2017 13h51	78.6493°N 9.6959°E	78.7919°N 7.0825°E
Transect 1a′	26/07/2017 13h51	27/07/2017 06h40	78.7919°N 7.0825°E	78.8794°N 6.7058°E
Transect 1b	31/07/2017 06h27	02/08/2017 15h19	78.8155°N 7.0135°E	78.6062°N 9.4520°E
Transect 1c	02/08/2017 15h19	04/08/2017 08h41	78.6062°N 9.4520°E	78.7963°N 7.0978°E
Transect 2a	27/07/2017 06h40	29/07/2017 08h04	78.8794°N 6.7058°E	79.0849°N 8.8190°E
Transect 2b	29/07/2017 08h04	31/07/2017 06h27	79.0849°N 8.8190°E	78.8155°N 7.0135°E
Transect 2c	04/08/2017 08h41	05/08/2017 06h10	78.7963°N 7.0978°E	78.9451°N 8.4855°E
Mooring	05/08/2017 06h10	06/08/2017 08h14	78.9451°N 8.4855°E	78.9624°N 8.5779°E
Transect 2c′	06/08/2017 08h14	07/08/2017 06h02	78.9624°N 8.5779°E	78.9878°N 9.5063°E

west of Svalbard: In this region, the Rossby radius of deformation is small (less than 10 km) and the spacing between moorings in the 79°N array and stations during hydrographic cruises (typically more than 5 km) can miss such mesoscale features.

In July 2017, a SeaExplorer glider was deployed on the shelf west of Svalbard offshore Kongsfjorden (Koenig et al., 2018). The glider crossed the slope west of Svalbard, both south and north of the Kongsfjorden opening (Figure 1a), crossing the WSC core six times. The glider documented the slope and shelf exchanges occurring in this area. The glider surfaced every 4 hr, with a distance of less than 5 km between each dive and sampled the fine mesoscale structure over the slope west of Svalbard, including lenses of cold waters in the core of the WSC, cascading along the slope and topographically trapped waves.

We investigate the processes observed in the glider data that might be contributing to the cooling of the WSC core. Section 2 presents the glider mission and data processing. Section 3 focuses on the observed lenses of cold waters, their structure, and their origin. Section 4 discusses the implication of the different processes identified in the cooling of the core of the WSC. Section 5 summarizes and concludes.

2. Glider Mission, Data, and Context

2.1. Glider Mission Overview

A SeaExporer glider developed by Alseamar in France was deployed from the R/V Lance on 24 July 2017 at 9.67°E, 78.65°N and recovered 14 days later on 7 August 2017 at 9.51°E, 79.00°N (Koenig et al., 2018). The glider repeated two transects three times, each across the western continental slope of Svalbard around the entrance of Kongsfjorden (Figure 1). Transect 1 is defined as the southern transect, south of Kongsfjorden, and transect 2 as the northern transect, north of Kongsfjorden. The westernmost limit of both transects (about 7°E, 78.8°N) was determined by the sea ice edge, which was over the outer Svalbard slope in July 2017. The glider also did a virtual mooring (repeat dives and ascents at nearly the same location) of about 24 hr at 400-m depth at the entrance of Kongsfjorden (data not used in this manuscript). Locations and dates of each transect can be found in Table 1 and Figure 1.

2.2. Glider Data Processing

The glider was equipped with a Glider Payload Conductivity Temperature Depth (GPCTD) from SeaBird, a dissolved oxygen sensor (Sea Bird SBE43F), and an optical sensor measuring Chlorophyll a (470/695 nm; data not used in this manuscript), colored dissolved organic matter (CDOM, 370/460 nm), and the total particle concentration or backscatter (backscattering at 700 nm; EcoPuck from Wetlabs; Koenig et al., 2018). The glider sampled the ocean along a sawtooth trajectory, from the surface down to a maximum depth of 700 m or the bottom if shallower than 700 m, with an average of 1.7 km between each surfacing location. As the isopycnal slopes are much smaller than the pitch angle of the glider, each up and down dives can be considered as vertical profiles. Over the 14 day-long mission, a total of 428 vertical profiles were made, covering a total of 375 km in horizontal distance.

We use hereafter the International Thermodynamic Equations of Seawater (TEOS-10) framework (McDougall et al., 2012) with conservative temperature (°C) and absolute salinity (g/kg).

Glider data were processed using the SOCIB toolbox (https://github.com/socib/ glider_toolbox). Thermal lag issues of the GPCTD probe were corrected by applying the method of Garau et al. (2011). The density was then despiked and interpolated, and salinity was recalculated from the temperature and the corrected density. Data were averaged on a 1-m vertical grid. Data from the glider were compared to the closest ship Conductivity Temperature Depth (CTD) data (in time and in space) performed during the accompanying research cruise (24 July to 8 August 2017 on the research vessel R/V Lance). The agreement between glider and ship CTD data is remarkable, ΔT about 0.005 °C, ΔS about 0.01 g/kg (not shown) and resulting glider data accuracy is estimated to be 0.005 °C for temperature and 0.01 g/kg for salinity.

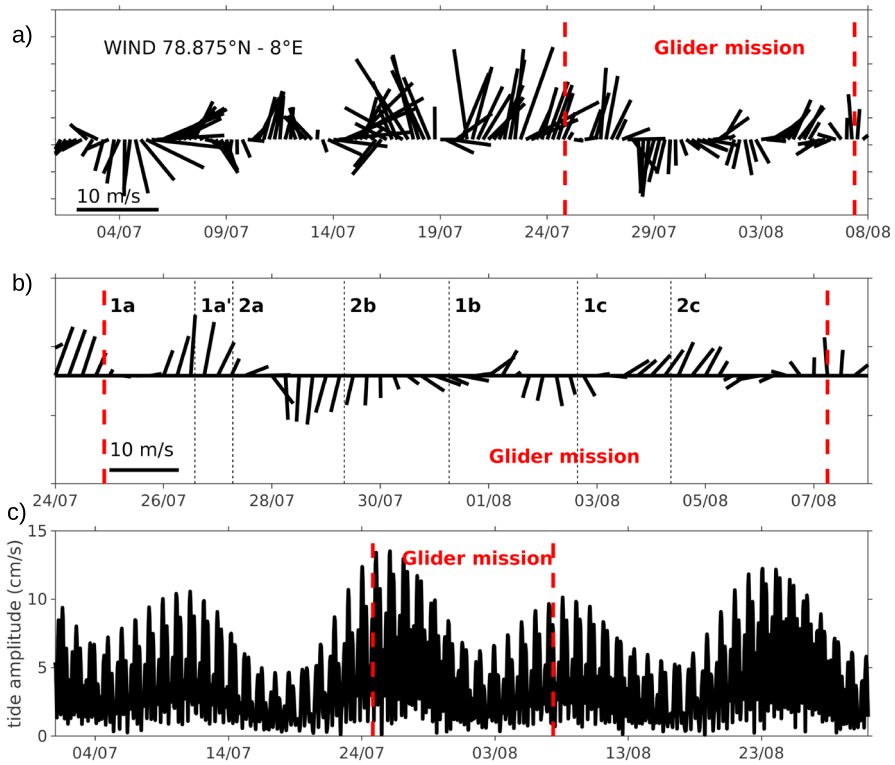

Figure 2. (a) Stickplot of the wind (m/s) at 10 m at 78.80°N to 8°E from June to August 2017. The red dashed lines delineates the period of the glider mission. (b) Close-up on the wind during the glider mission. (c) Barotropic tide velocity amplitude (cm/s) at 78.80°N to 8°E deduced from AOTIM-5.

CDOM and total particle concentration are presented with appropriate sensor calibration and are respectively given in parts per billion (ppb), per meter per steradian ($m^{-1}{\cdot}sr^{-1}$).

Depth-averaged currents over each glider dive were computed from the dead-reckoning navigation of the glider and GPS fixes at the surface. Baroclinic geostrophic velocities v_g have been calculated from the glider density data applying the thermal wind formula:

$$\delta_z v_g = -g/f \cdot \delta_x(\sigma/\sigma_0) \quad (1)$$

with σ the potential density, σ_0 a reference density taken as 1,024 kg/m^3, g the gravitational constant, and f the Coriolis parameter. For this, the density field has been smoothed with a running mean over three profiles. Baroclinic velocities are computed with a nil average on each profile.

2.3. Wind Data and Tide Model

In addition to the glider data, we use 10-m wind reanalysis data from the daily European Centre for Medium range Weather forecasts (ECMWF) reanalysis outputs (http://apps.ecmwf.int/datasets/data/interim-fulldaily/levtype=sfc/) and tidal currents from the Arctic Ocean Tidal Inverse Model (AOTIM-5; Padman & Erofeeva, 2004). Using AOTIM-5 we estimate the tidal current velocities associated with the eight most energetic tidal components (M2, S2, N2, K2, O1, K1, P1, and Q1; Figure 2c). The model provides barotropic tidal velocities on a 5-km horizontal resolution grid. We updated the bathymetry of the model with International Bathymetric Chart of the Arctic Ocean (https://www.ngdc.noaa.gov/mgg/bathymetry /arctic /arctic.html).

2.4. Regional Context

The glider transects 1 and 2 are located just north and south of the Fram Strait mooring array (Figure 1b, orange stars), maintained for more than 20 years by the Alfred Wegener Institute on this side of the strait.

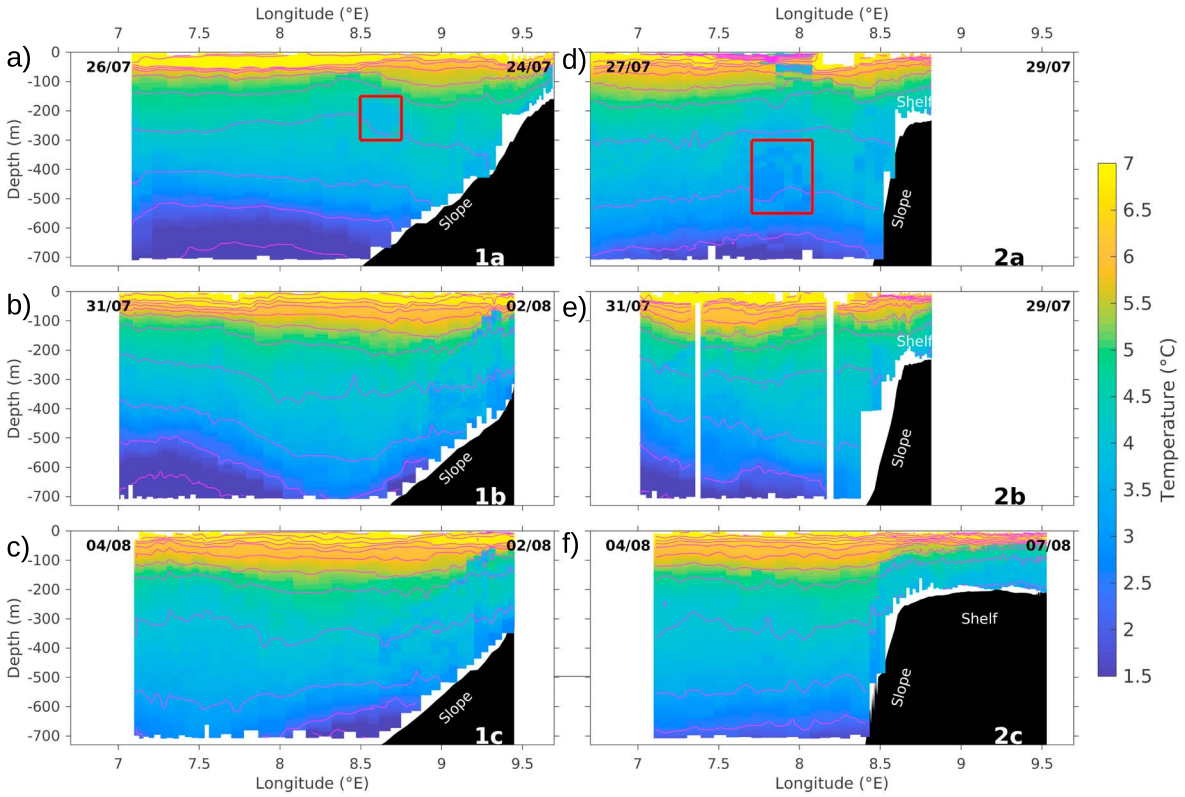

Figure 3. Conservative temperature (°C) for each glider transect. (a) Transects 1a, (b) 1b, (c) 1c, (d) 2a, (e) 2b, (f) 2c, and 2c′. Magenta lines are isopycnals every 0.06 kg/m^3.

Data analysis from the Fram Strait mooring array has shown that topographically trapped waves with periods between hours and days are found in this area (Nilsen et al., 2016).

The wind regime during the glider mission was favorable for shelf/slope exchanges (Figure 2). Northerly winds occurring at several times during the glider mission, such as on 28 and 29 July, could favor cascading of water from the shelf down the slope (Goszczko et al., 2018).

The barotropic tide (Figure 2c) was strong (maximum amplitude 12 cm/s) at the beginning of the glider mission and potentially generating topographically trapped waves (Nilsen et al., 2006).

All the glider transects cross the WSC core. On all transects, temperature decreases with depth (Figure 3), from 7 °C in the mixed layer, to temperature still larger than 3 °C at 500 m, indicating AW presence. On the shelf, waters are colder than on the slope (about 4 °C at 150 m on the shelf, compared to 5.5 °C on the slope, see transect 2c in Figure 3, for example). The WSC and waters on the shelf are separated by a strong temperature and salinity gradient, and almost no density gradient, in agreement with findings by Saloranta and Svendsen (2001).

Going into more details, there are many differences between transects. Transects 2a–2c are on a steeper slope than transects 1a–1c, which may have consequences for the shelf/slope exchanges. The glider transects are characterized by large variability: Although they took place within a 14-day period, some features are visible in individual transects only. Large differences are observed between transects 1b and 1c although they are completed less than 2 days apart: The base of the AW layer, around the isotherm 3 °C, depicts a deepening near 8.6°E in transect 1b, while this deepening is shifted westward to 7.5°E in transect 1c. The processes likely responsible for these observations are discussed in section 4.

Transects 1a and 2a show two remarkable small lenses of colder water in the WSC. The next section focuses on these two small features.

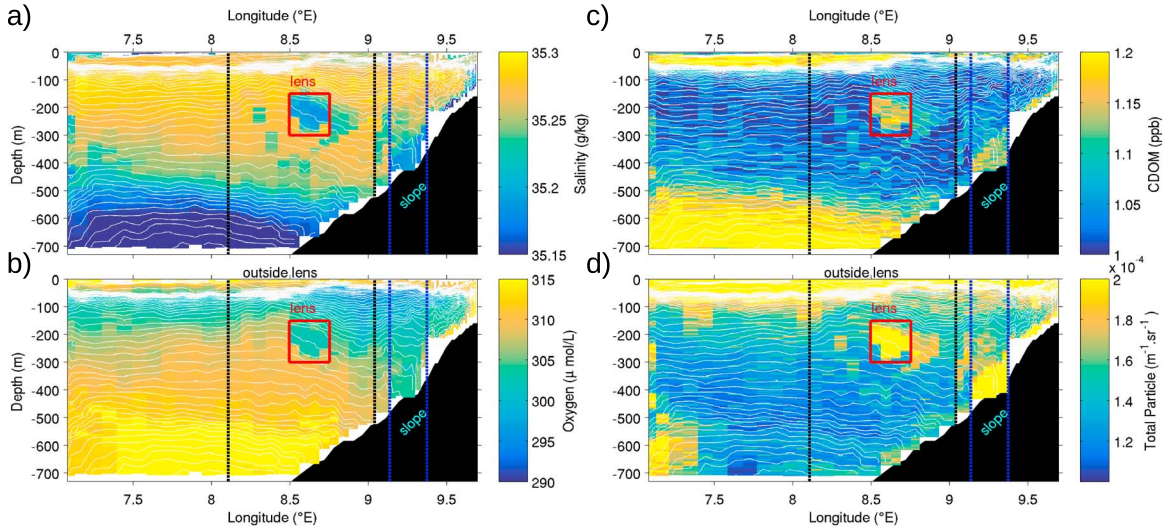

Figure 4. Measured parameters for transect 1a. (a) Absolute salinity (g/kg). (b) Dissolved oxygen (μmol/L). (c) CDOM (ppb). (d) Total particle concentration (m^{-1}·sr^{-1}). The red box delimits the lens; the black dashed lines, the area considered as outside the lens (except the profiles that are in the red box); and the blue dashed lines, the area considered as the slope. White lines are isopycnals every 0.01 kg/m^3. Black shading is topography. CDOM = colored dissolved organic matter; ppb = parts per billion.

3. Cold and Fresh Lenses

3.1. Cold and Fresh Lens in Transect 1a

Transect 1a, from near the shelf break (9.70°E, 78.65°N) and across the upper part of the slope (7.08°E, 78.79°N), lasted less than 2 days (Table 1). The first cold-water lens we study was found around 8.66°E, 78.71°N, on the slope over 600- to 700-m depth (Figure 4, red box). It was sampled over two dives (four slanted profiles), corresponding to a total horizontal distance of 4.2 km. The structure was located between 150- and 300-m depth, with a core at 225-m depth. The aspect ratio (vertical/horizontal) is then about 1/20, which is why we chose to refer to it as a lens. Compared to the surrounding waters, the lens is cold (3.79 °C compared to 4.46 °C in surrounding waters) and fresh (35.19 g/kg compared to 35.26 g/kg in surrounding waters), associated with a divergence of the isopycnals (Figure 4, white lines). This structure is also depleted in dissolved oxygen (302 vs. 305 μmol/L) and enriched in CDOM (1.14 vs. 1.04 ppb) and in total particle concentration (2.1×10^{-4} vs. 1.5×10^{-4} m^{-1}·sr^{-1}). The structure is well mixed, with no stratification (Brunt-Väisälä frequency plots, not shown and Figure 4d). Similar water properties to this lens are found in the waters close to the bottom on the upper slope (blue profiles in Figure 5), as observed in the T-S diagram (Figure 5g): Waters from the bottom of the upper slope and of the lens have identical temperature, salinity, and density. These waters are found on the slope at around 370–420 m, about 150 m deeper than the lens structure. Along transect 1a, waters over the bottom of the slope and in the lens are located on the same isopycnals (Figures 4 and 5d). From these observations, we infer that the lens and the waters over the bottom of the upper slope have a common origin.

Depth-averaged currents deduced from the glider trajectory are much larger than the predicted barotropic tide from the AOTIM-5 (Padman & Erofeeva, 2004, and Figure 6). Once the depth-averaged currents are detided, northward velocities of more than 10 cm/s are observed on two thirds of the transect (from the shelf to 7.3°E), corresponding to the WSC core (Beszczynska-Möller et al., 2012, and Figure 6a). West of 7.3°E, currents turn to the southwest, possibly the signature of eddies or of the AW recirculation in Fram Strait (Hattermann et al., 2016; Håvik et al., 2017; Von Appen et al., 2016).

The baroclinic current deduced from the density field is smaller by an order of magnitude than the depth-averaged current (Figure 6). Baroclinic velocities in the lens (red dashed box in Figure 6) describe a slightly anticyclonic structure, with a horizontal velocity difference of about 2 cm/s between the two sides of the structure. The Rossby radius of deformation in the area is around 3–4 km (Von Appen et al., 2016), and the horizontal extent of the observed lens was about 4 km. The glider transect might thus have passed

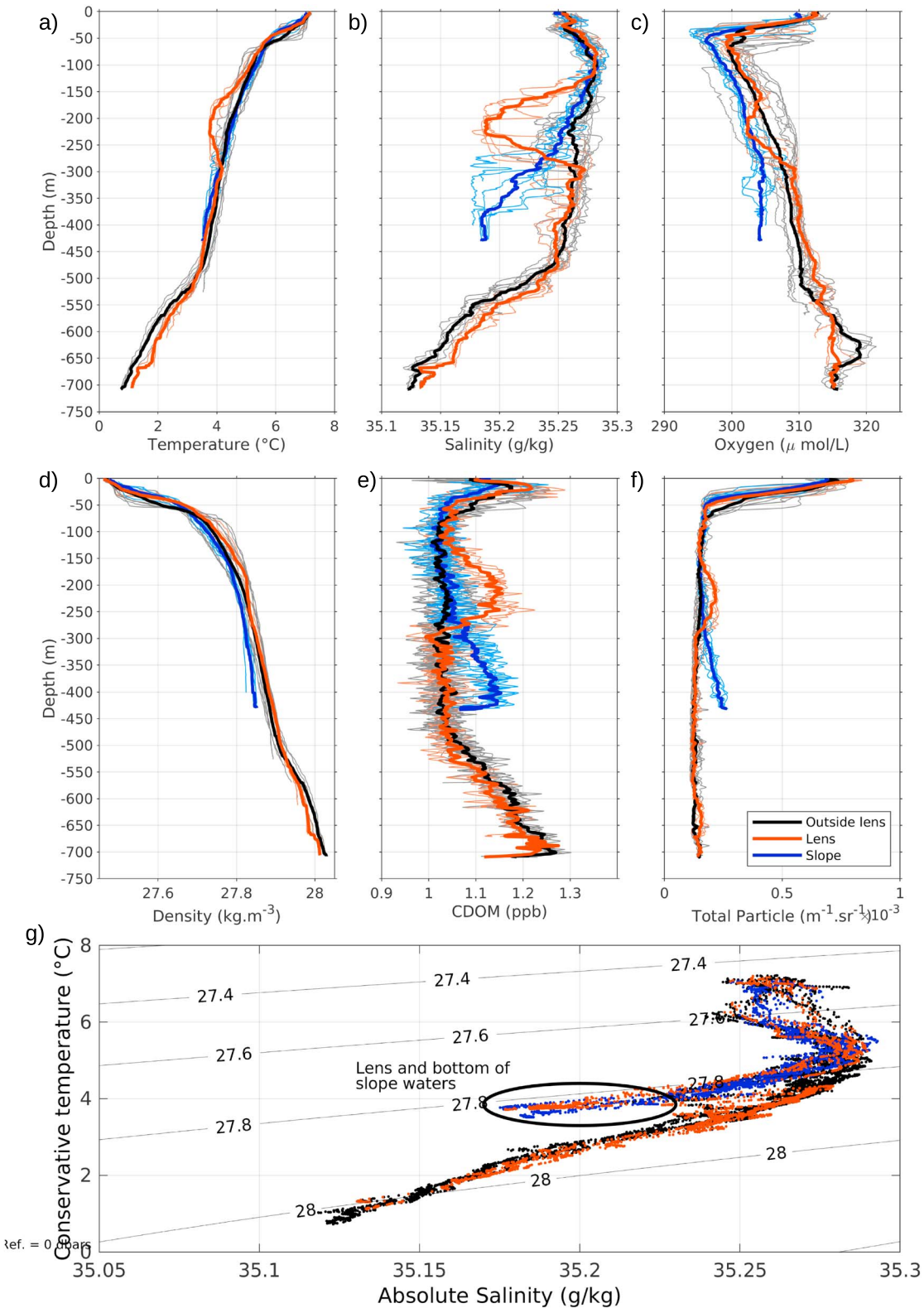

Figure 5. Vertical profiles of (a) conservative temperature (°C), (b) absolute salinity (g/kg), (c) dissolved oxygen (μmol/L), (d) potential density (kg/m^3), (e) CDOM (ppb), and (f) total particle concentration (m^{-1}·sr^{-1}) in the vicinity of the lens observed in transect 1a. In red, profiles located inside the lens (corresponding to the red box in Figure 4). In black profiles outside the lens, corresponding to profiles inside the black lines in Figure 4, except for the ones in the red box. In blue, profiles from the slope, which are profiles between the blue lines in Figure 4. Thick lines correspond to the mean profile for each area (average of thin profiles). (g) T-S diagram in the vicinity of the lens observed in transect 1a. Same color code as the above panels. CDOM = colored dissolved organic matter; ppb = parts per billion.

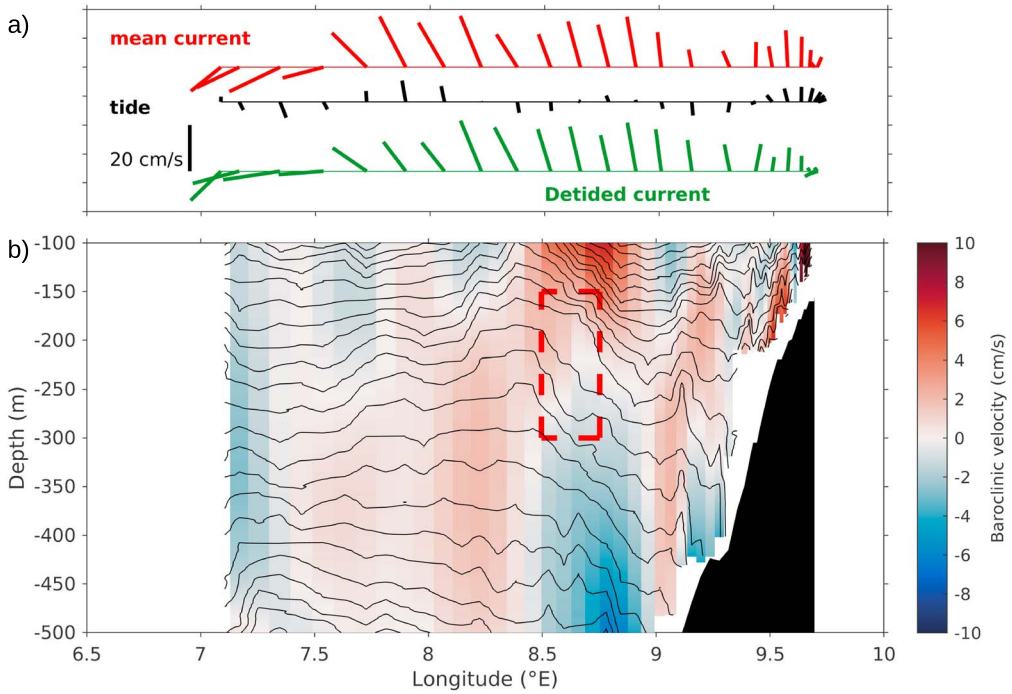

Figure 6. (a) In red: dive-averaged mean current (cm/s) as estimated by the glider along transect 1a. In dark: tide velocity along transect 1a estimated by the barotropic tidal model AOTIM-5 (cm/s). In green: the detided current deduced from the dive-averaged mean current and the tide velocities (cm/s). (b) Close-up (100- to 500-m depth) of the baroclinic geostrophic velocity (cm/s) along transect 1a deduced using the thermal wind equation from the density field of the glider. Each profile is referenced with a mean average of 0. The red box indicates the location of the lens. Black lines are isopycnals.

through the lens somewhere between its center and its edge. The lens is located on the outer side of the WSC (700-m isobath) where the current is known to be barotropically unstable (Von Appen et al., 2016). This instability could have helped to put these lenses on the outside of the slope.

A similar lens discussed in the next section was observed in transect 2a, although slightly deeper and further offshore.

3.2. Cold and Fresh Lens in Transect 2a

Transect 2a, where the second lens is observed, was made from the slope (6.71°E, 78.88°N) toward the shelf (8.82°E, 79.08°N) and lasted about 2 days (Table 1). The lens was cold and fresh like the first one and found on the slope over 1,100- to 1,200-m depth (around 7.78°E, 79.01°N, Table 2; Figure 7, red box). The core of the lens was visible in four dives (eight slanted profiles), corresponding to a horizontal distance of about 8 km. The lens was located between 300- and 550-m depth, with a core at about 400-m depth and has a similar aspect ratio as the lens found in transect 1a, about one twentieth.

Compared to surrounding waters, the lens in transect 2a was cold (3.21 °C vs. 3.75 °C) and fresh (35.19 g/kg vs. 35.26 g/kg). This lens was enriched in CDOM (1.18 vs. 1.07 ppb) and in total particle concentration ($2.4.10^{-4}$ vs. $1.3.10^{-4}$ $m^{-1}.sr^{-1}$) and had similar characteristics to water masses found close to the bottom on the slope, suggesting a common origin (Figure 8). The differences between the shelf waters and the lens could be explained by the fact that on this transect, the shelf that is sampled is located further north than the lens. If we assume that these two water masses have a common origin, the lens probably originates from the shelf further south than the outer shelf sampled by the glider on transect 2a. The lens, traveling northward and offshore, would thus be subject to modification processes and is not directly linked to the shelf bottom waters observed on the transect.

Along transect 2a, the depth-averaged current was mostly oriented south (Figure 9a). This is in contradiction with the general picture of the current in this area, as the WSC typically flows to the north. At the location of the core of WSC, the current was weakly oriented to the north. Such south-flowing currents on the Svalbard

Table 2
Characteristics of the Cold Core Lenses Found in Transects 1a and 2a

	Lens in transect 1a	Lens in transect 2a
Number of profiles	4	8
Time (UTC)	25/07/2017 14h30–17h23	28/07/2017 09h55–16h20
Latitude	78.71°N	79.01°N
Longitude	8.66°E	7.78°E
Depth (m)	150–300	300–550
Core depth (m)	225	400
Bottom depth (m)	600–700	1,100–1,200
Diameter (as observed, km)	4.2	7.12
Core/surrounding temperature (°C)	3.79/4.46	3.21/3.75
Core/surrounding salinity (g/kg)	35.19/35.26	35.19/35.25
Core/surrounding Chloro (μg/L)	0/0	0/0
Core/surrounding CDOM (ppb)	1.14/1.04	1.18/1.07
Core/surrounding Backscatter (10^{-4} m^{-1}·sr^{-1})	2.1/1.5	2.4/1.3
Core/surrounding oxygen (μmol/L)	302/305	310/310

slope intermittently occur as documented by the Fram Strait mooring array (Beszczynska-Möller et al., 2015). These events could indicate the presence of localized recirculation cells and eddies affecting the *classical* northward flow regime of the WSC. Nilsen et al. (2006) also noticed that the current meter time series located on the West Spitsbergen Slope contain rotating energy on short and long periods (hours to days). The baroclinic geostrophic velocities deduced from the density field show a velocity difference of about 4–5 cm/s at the lens location (Figure 9b).

Compared to the lens found in transect 1a, the lens in transect 2a is on a deeper horizon (400 vs. 225 m) and is thicker (250 vs. 150 m). The lens in transect 2a is also slightly further offshore (7.7°E vs. 8.6°E and over a deeper bottom depth 1,100 vs. 700 m). The lens in transect 2a is less homogeneous in the vertical, probably due to mixing with surrounding waters. All these elements suggest that the cold core lens in transect 2a has been in the WSC core for a longer period of time than the cold core lens in transect 1a.

4. Discussion

4.1. Generation of the Cold Core Lenses

Two cold core lenses are documented about 39 km apart and nearly 3 days apart. If we have crossed the same lens twice, it would equate to a horizontal displacement of the lens of 15 cm/s with a northward and offshore

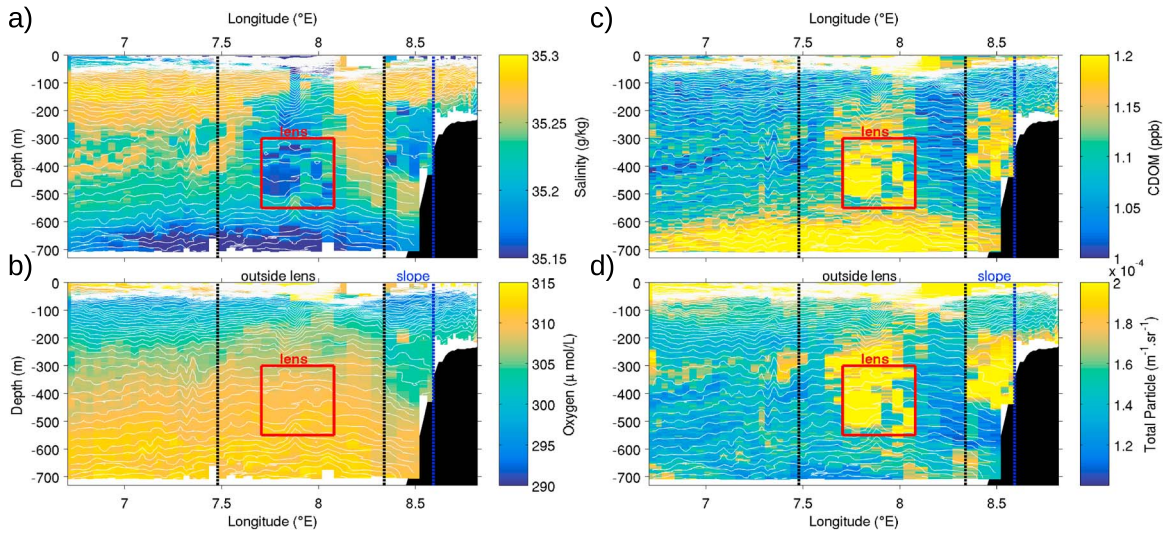

Figure 7. Same as Figure 4 but for transect 2a. CDOM = colored dissolved organic matter; ppb = parts per billion.

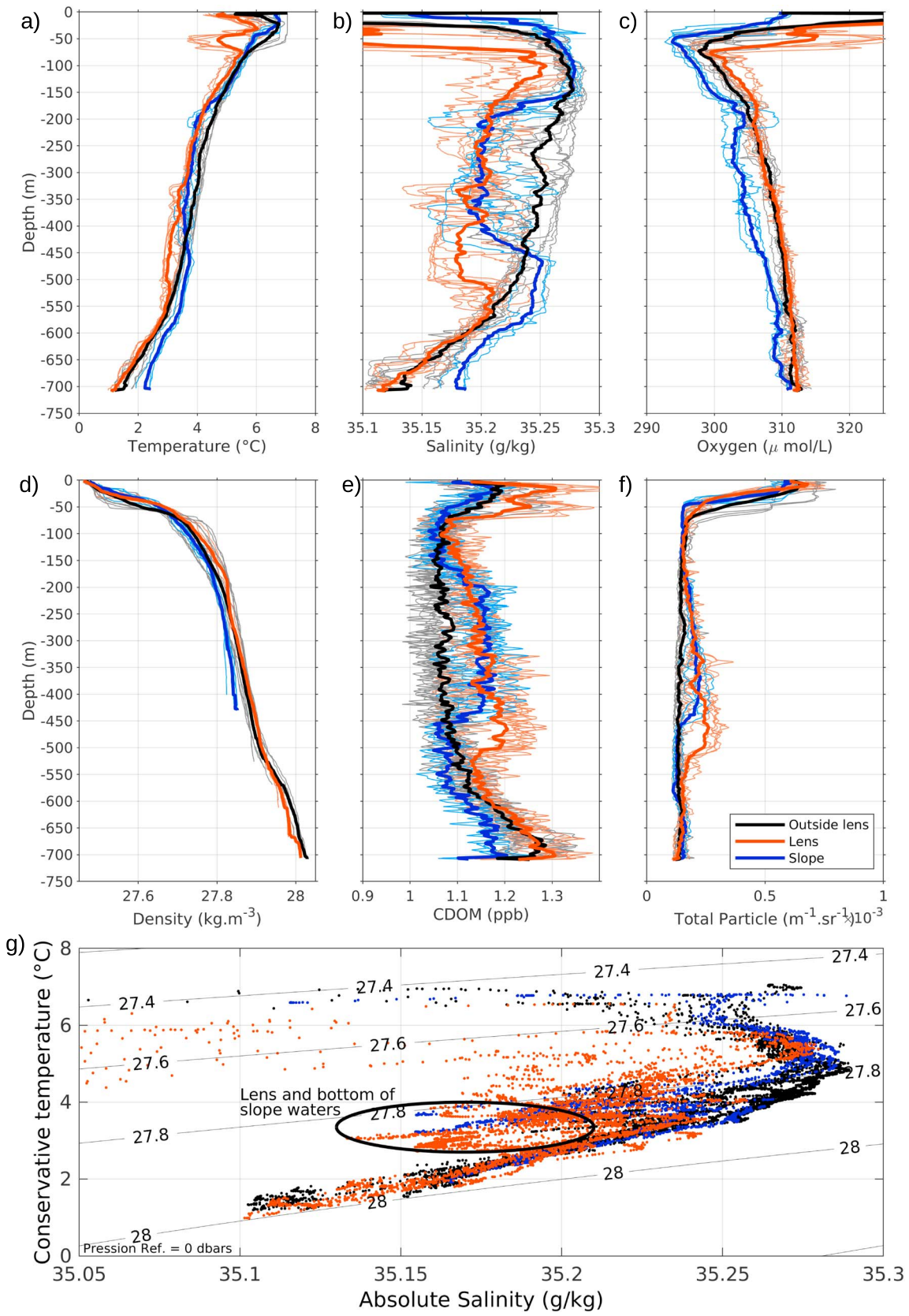

Figure 8. Same as Figure 5 but for transect 2a. CDOM = colored dissolved organic matter; ppb = parts per billion.

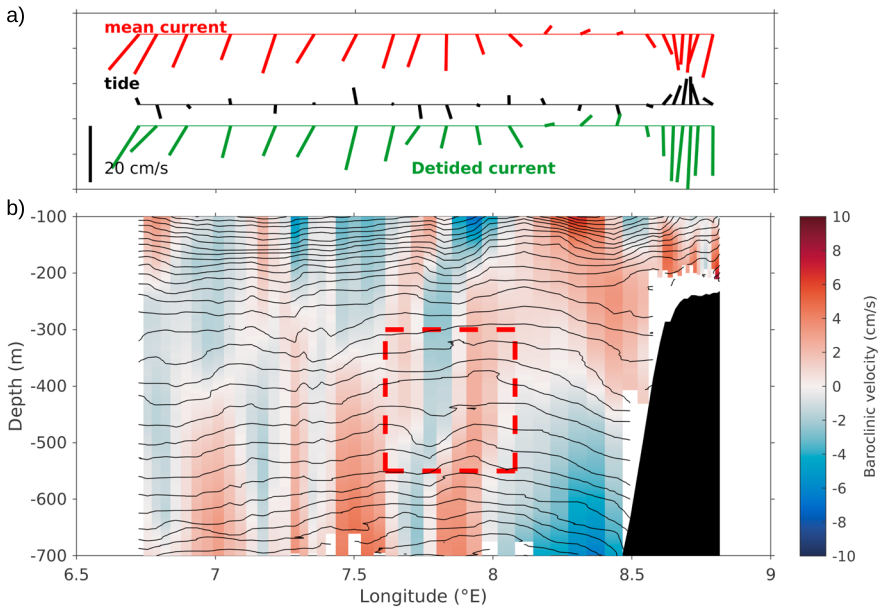

Figure 9. (a) Same as Figure 6 but for transect 2a. (b) The close-up is from 100- to 700-m depth.

component. In this calculation we did not take into account the vertical displacement that would have occurred (from 225-m depth in transect 1a to 400-m depth in transect 2a). This velocity is larger (about 5 times) than the eddy translational velocities estimated from a high-resolution ocean model in the AW inflow north of Svalbard in Crews et al. (2017) of about 3.5 cm/s. We could expect the eddy translational velocities to be slightly smaller north of Svalbard compared to the WSC as the current is less energetic (current speed about 40 cm/s in the WSC and about 30 cm/s in the AW inflow north of Svalbard, Perez-Hernandez et al., 2017). The second lens has slightly different properties compared to the first one: colder (3.21 °C vs. 3.79 °C) and deeper (400 vs. 225 m; Table 1). We therefore hypothesize that two distinct lenses were sampled.

The two consecutive southern glider transects on the same track (1b and 1c, Figure 1b) show cascading of waters along the slope, from about 100- to 300-m depth (Figures 3b and 3c). In transect 1b, the cascading is noticeable offshore up to 8.9°E. The cascading in 1c, sampled less than 20 hr later is more advanced and is visible as far west as 8.6°E. Similar cascading patterns are visible in the salinity observations (not shown), with propagation of fresh waters from the shelf down to the slope. A horizontal propagation velocity of the cascading can be estimated as the end of the cascading is farther offshore in transect 1c than in transect 1b. We found a propagation speed of about 8.2 cm/s. The slope in transects 1b and 1c is quite gentle compared to transects 2a–2c where it is very steep. (Figure 3). Transect 2c also suggests the flow of water from the shelf along the steep slope as deep as 500-m depth. However, no propagation speed can be estimated on the northern transect and on the steeper slope as the trajectories of the transects are not strictly identical (Figure 1b).

Cascading of cold and fresh waters down a slope has been documented in other regions. For example, Falina et al., (2012) documented cascading of dense shelf waters in the Irminger Sea down to 3,000-m depth. These episodes were intermittent and occurred at all seasons of the year.

The observed cascading associated with a diapycnal displacement of the waters from the shelf down the slope is consistent with the temperature-salinity diagram of waters from the shelf at the end of transect 2c (Figure 10). Waters found on the shelf are warmer and saltier than waters from the fjord and from the Spitsbergen Polar Current: 35.13 g/kg and about 3.8 °C compared to the Arctic Waters with $-1.5 < T < 1$ °C and $34.5 < S < 34.9$ g/kg (Tverberg et al., 2014). These shelf waters are quite close to the WSC core properties ($3 < T < 4$ °C, $35.2 < S < 35.4$ g/kg, Tverberg et al., 2014), although slightly colder and fresher. The presence of these shelf waters with WSC properties in our observations could be explained by the *Spitsbergen Trough Current* (Nilsen et al., 2016). This current originates from AW intrusions on the West Spitsbergen Shelf when southerly wind and Ekman transport push water onto the shelf.

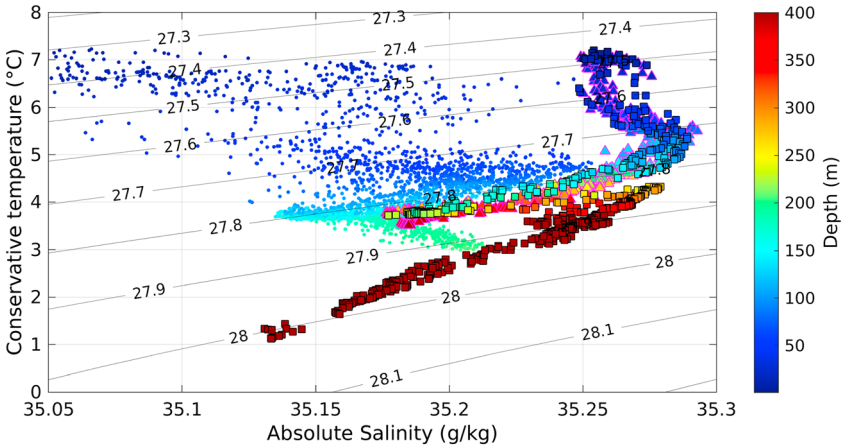

Figure 10. Conservative temperature (°C). Absolute salinity (g/kg) diagram color-coded with depth (m). Squares with black edges are from profiles in the cold core lens from transect 1a (see Figure 3). Triangles with magenta edges are from profiles on the slope (see Figure 3). Small dots without edge are from profiles on the shelf (transect 2c′).

Waters from the lens in transect 1a have similar temperature and salinity characteristics to the ones on the slope (Figure 10, squares and triangles, respectively). Waters on the slope and in the lens (squares and triangles in Figure 10) are saltier (35.19 g/kg) than waters found on the shelf (dots, 35.13 g/kg). Moreover, the lens has a core at 225-m depth, shallower/deeper than the depth where the waters with similar properties on the shelf/slope are found (150- and 400-m depth, respectively). Salinity differences are due to mixing of the shelf waters with the WSC surrounding waters on the slope and depth differences are due to the cascading of shelf waters along the continental slope.

4.2. Topographically Trapped Waves

The 3 °C isotherm shows a maximum depth of 600–700 m. The location of the maximum varies in the three repeats of the southernmost transects 1a–1c (Figure 3, thick magenta contour) and seems to shift offshore from transect 1b to 1c from 8.36°E to 7.5°E (Figures 3c and 3e). This shift could be explained by the northward propagation of topographically trapped waves excited by the passage of weather systems (e.g., Inall et al., 2015; Nilsen et al., 2006) such as the strong southerly winds observed at the beginning of July 2017 during the glider mission (Figure 2a). Southerly winds create a convergence of the surface Ekman flow toward the coast, which leads to an assumed depression of the thermocline. This perturbation is at the origin of the northward propagation of topographically trapped waves. These waves could potentially contribute significantly to the volume exchange of water along the slope (Inall et al., 2015). Topographically trapped waves and cold and fresh lenses probably interact. Further analysis of such coastally trapped waves and their interaction with the shelf break and lenses is difficult with this limited data set.

4.3. Implications for the Cooling of the WSC

Rough estimates of heat content (HC), freshwater content (FWC), and CDOM content (CDOMC) have been computed for the two observed lenses:

$$HC = \int \rho Cp(T - T_{\text{ref}})\mathrm{d}V, \tag{2}$$

$$FWC = \int \frac{(S - S_{\text{ref}})}{S_{\text{ref}}}\mathrm{d}V, \tag{3}$$

$$CDOMC = \int (CDOM - CDOM_{\text{ref}})\mathrm{d}V, \tag{4}$$

with ρ the mean density of the seawater (here 1,024 kg/m^3) and Cp is the specific heat of seawater. We assume that each lens is a cylinder of diameter twice the observed horizontal extent of the lens (9 km for lens 1a and 16 km for lens 2a). Taking the surrounding water as the reference (T_{ref} = 4.387 °C, S_{ref} = 35.26 g/kg, $CDOM_{\text{ref}}$ = 1.04 ppb for transect 1a; T_{ref} = 4.382 °C, S_{ref} = 35.26 g/kg, $CDOM_{\text{ref}}$ = 1.07 ppb for transect 2a), we found that lenses in transects 1a and 1b have anomalous HC of respectively -3×10^{15} and

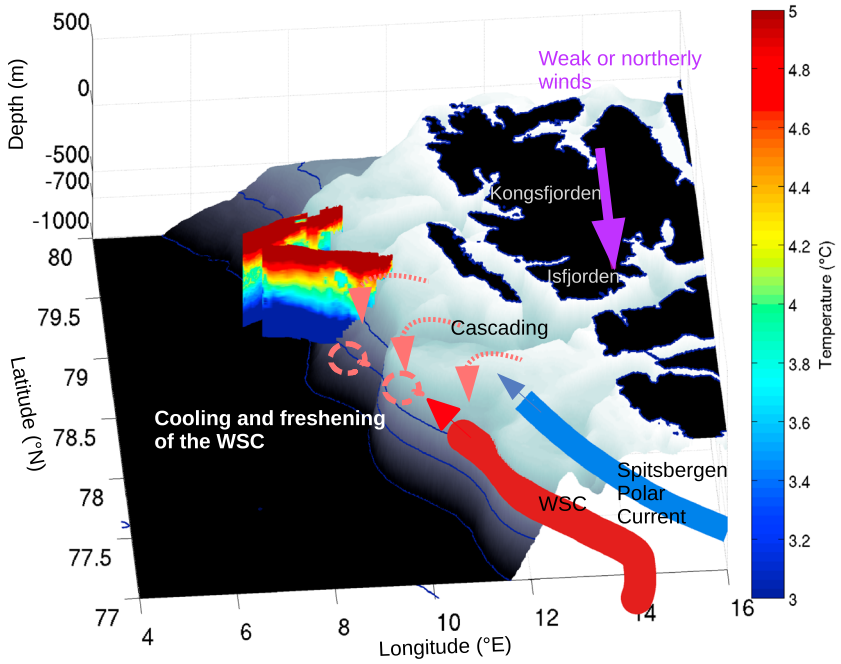

Figure 11. Schematic of the slope-shelf exchanges documented by the SeaExplorer glider. A relaxing state with weak winds is characterized by cascading of relatively cold water from the shelf down the slope and cold core eddies in the WSC. WSC = West Spitsbergen Current.

-18×10^{15} J. The FWC anomaly is respectively 2.68×10^{6} and 15×10^{6} m^3. Compared to the AW in the WSC, eddies are enriched in CDOM, with a CDOM anomaly content of respectively 1.45×10^{8} and 9×10^{8} ppb·m^3. These cold-water lenses that slowly mix with WSC waters could therefore be a source of dissolved organic matter for the Arctic Ocean as they transport dissolved organic matter from the shelf into the WSC. Their influence has yet to be quantified.

As highlighted by Boyd and D'Asaro (1994), one way of cooling the WSC is from the surface to either the air or sea ice; however, the magnitude of surface cooling is too small to explain the overall cooling of the WSC. By transporting cold fresh waters from the Svalbard shelf into the WSC, the lenses crossed in transects 1a and 2a participate in the cooling and freshening of the WSC as it flows northward along the western shelf of Svalbard, impacting its properties as it enters the Arctic. The snapshots from the glider data are not sufficient to estimate the longer-term contribution of these lenses to the cooling of the WSC core. Similar observations in the Irminger Sea estimated that even if such cascading events are of short duration, the contribution of a single event to the deep current volume could be as large as 25% (Falina et al., 2012).

5. Conclusions

The SeaExplorer glider proved to be reliable as far north as 79°N, despite large current velocities. The glider data with very high spatial and vertical sampling frequency, provided valuable information on mesoscale patterns of less than 10 km.

The cooling process of the WSC through cascading shelf waters and lens features observed in the glider data is summarized in Figure 11, which shows the relaxing state when southerly winds shift to northerly or weak winds. Waters that have accumulated on the shelf during periods of southerly winds cascade down the slope when northerly or weak winds blow, and small cold core lenses detach in the outer part of the WSC that is known to be unstable baroclinically (Von Appen et al., 2016).

The cold core lenses documented in this study are one mechanism that cools the WSC core but several other processes regulate the cooling of the WSC: the seasonality of the WSC, tides, coastally trapped waves, exchanges with the surface and with offshore waters, and the sea ice extent (e.g., Boyd & d'Asaro, 1994; Nilsen et al., 2006; Saloranta & Haugan, 2004). The lenses presented here were observed in summer, when

the WSC is slower than in autumn and winter (volume transport 1 Sv compared to 5 Sv, respectively, Beszczynska-Möller et al., 2012). Nilsen et al. (2016, their figure 8) show a seasonality in the along-coast wind stress, with positive wind stress in autumn and winter and negative in spring and summer. This seasonality could result in a preference of upwelling of warm AW on the slope in winter and a cascading of shelf water down the slope in summer. We could then speculate that these lenses are mainly present in summer, although summer has been described as a period of weak eddy kinetic energy (Von Appen et al., 2016). These lenses would then play a role in cooling the core of the WSC mainly in summer.

Acknowledgments
The glider work was supported by the European project ACCESS. We thank Norwegian Polar Institute and the captain and crew on board the R/V Lance for the logistics of the glider deployment and recovery. We also thank all the glider pilots from Alseamar. Z. Koenig acknowledges a post doc funding from the Pan-Arctic Option Belmont Forum. A. Meyer was supported by the Australian Research Council Centre of Excellence for Climate Extremes (CE170100023) and by the Norwegian Polar Institute's Centre for Ice, Climate and Ecosystems. A. Sundfjord acknowledges the Fram Centre *Arctic Ocean* project A-TWAIN for funding. The glider data are publicly available in the SEANOE database: http://doi.org/10.17882/56366.

References

Beszczynska-Möller, A., Fahrbach, E., Schauer, U., & Hansen, E. (2012). Variability in Atlantic water temperature and transport at the entrance to the Arctic Ocean, 1997–2010. *ICES Journal of Marine Science*, *69*(5), 852–863. https://doi.org/10.1093/icesjms/fss056

Beszczynska-Möller, A., von Appen, W.-J., & Fahrbach, E. (2015). Physical Oceanography and Current meter data from moorings F1–F14 and F15/F16 in the Fram Strait, 1997–2012. *PANGAEA*. https://doi.org/10.1594/PANGAEA.150016

Boyd, T. J., & D'Asaro, E. A. (1994). Cooling of the West Spitsbergen Current: Wintertime observations west of Svalbard. *Journal of Geophysical Research*, *99*(C11), 22,597–22,618. https://doi.org/10.1029/94JC01824

Cottier, F. R., Nilsen, F., Inall, M. E., Gerland, S., Tverberg, V., & Svendsen, H. (2007). Wintertime warming of an Arctic shelf in response to large-scale atmospheric circulation. *Geophysical Research Letters*, *34*, L10607. https://doi.org/10.1029/2007GL029948

Crews, L., Sundfjord, A., Albretsen, J., & Hattermann, T. (2017). Mesoscale eddy activity and transport in the Atlantic Water inflow region north of Svalbard. *Journal of Geophysical Research: Oceans*, *123*, 201–215. https://doi.org/10.1002/2017JC013198

Falina, A., Sarafanov, A., Mercier, H., Lherminier, P., Sokov, A., & Daniault, N. (2012). On the cascading of dense shelf waters in the Irminger Sea. *Journal of Physical Oceanography*, *42*(12), 2254–2267. https://doi.org/10.1175/JPO-D-12.012.1

Garau, B., Ruiz, S., Zhang, W. G., Pascual, A., Heslop, E., Kerfoot, J., & Tintoré, J. (2011). Thermal lag correction on Slocum CTD glider data. *Journal of Atmospheric and Oceanic Technology*, *28*(9), 1065–1071. https://doi.org/10.1175/JTECH-D-10-05030.1

Goszczko, I., Ingvaldsen, R. B., & Onarheim, I. H. (2018). Wind-driven cross-shelf exchange-West Spitsbergen Current as a source of heat and salt for the adjacent shelf in Arctic winters. *Journal of Geophysical Research: Oceans*, *123*, 2668–2696. https://doi.org/10.1002/2017JC013553

Hattermann, T., Isachsen, P. E., von Appen, W.-J., Albretsen, J., & Sundfjord, A. (2016). Eddy-driven recirculation of Atlantic Water in Fram Strait. *Geophysical Research Letters*, *43*, 3406–3414. https://doi.org/10.1002/2016GL068323

Håvik, L., Pickart, R. S., Våge, K., Torres, D., Thurnherr, A. M., Beszczynska-Möller, A., et al. (2017). Evolution of the East Greenland Current from Fram Strait to Denmark Strait: Synoptic measurements from summer 2012. *Journal of Geophysical Research: Oceans*, *122*, 1974–1994. https://doi.org/10.1002/2016JC012228

Inall, M. E., Nilsen, F., Cottier, F. R., & Daae, R. (2015). Shelf/fjord exchange driven by coastal-trapped waves in the Arctic. *Journal of Geophysical Research: Oceans*, *120*, 8283–8303. https://doi.org/10.1002/2015JC011277

Koenig, Z., Beguery, L., Provost, C., Meyer, A., Sundfjord, A., Athanase, M., & Gascard, J.-C. (2018). SeaExplorer glider SEA028 observations west of Svalbard in July 2017. *SEANOE*. https://doi.org/10.17882/56366

McDougall, T. J., Jackett, D. R., Millero, F. J., Pawlowicz, R., & Barker, P. M. (2012). A global algorithm for estimating absolute salinity. *Ocean Science*, *8*(6), 1123–1134. https://doi.org/10.5194/os-8-1123-2012

Nilsen, F., Gjevik, B., & Schauer, U. (2006). Cooling of the West Spitsbergen Current: Isopycnal diffusion by topographic vorticity waves. *Journal of Geophysical Research*, *111*, C08012. https://doi.org/10.1029/2005JC002991

Nilsen, F., Skogseth, R., Vaardal-Lunde, J., & Inall, M. (2016). A simple shelf circulation model: Intrusion of Atlantic water on the West Spitsbergen shelf. *Journal of Physical Oceanography*, *46*(4), 1209–1230. https://doi.org/10.1175/JPO-D-15-0058.1

Padman, L., & Erofeeva, S. (2004). A barotropic inverse tidal model for the Arctic Ocean. *Geophysical Research Letters*, *31*, L02303. https://doi.org/10.1029/2003GL019003

Perez-Hernandez, M. D., Pickart, R. S., Pavlov, V., Våge, K., Ingvaldsen, R., Sundfjord, A., et al. (2017). The Atlantic Water boundary current north of Svalbard in late summer. *Journal of Geophysical Research: Oceans*, *122*, 2269–2290. https://doi.org/10.1002/2016JC012486

Saloranta, T. M., & Haugan, P. M. (2004). Northward cooling and freshening of the warm core of the West Spitsbergen Current. *Polar Research*, *23*(1), 79–88. https://doi.org/10.3402/polar.v23i1.6268

Saloranta, T. M., & Svendsen, H. (2001). Across the Arctic front west of Spitsbergen: High-resolution CTD sections from 1998–2000. *Polar Research*, *20*(2), 177–184. https://doi.org/10.3402/polar.v20i2.6515

Tverberg, V., & Nøst, O. A. (2009). Eddy overturning across a shelf edge front: Kongsfjorden, West Spitsbergen. *Journal of Geophysical Research*, *114*, C04024. https://doi.org/10.1029/2008JC005106

Tverberg, V., Nøst, O. A., Lydersen, C., & Kovacs, K. M. (2014). Winter sea ice melting in the Atlantic Water subduction area, Svalbard Norway. *Journal of Geophysical Research: Oceans*, *119*, 5945–5967. https://doi.org/10.1002/2014JC010013

Von Appen, W.-J., Schauer, U., Hattermann, T., & Beszczynska-Möller, A. (2016). Seasonal cycle of mesoscale instability of the West Spitsbergen Current. *Journal of Physical Oceanography*, *46*(4), 1231–1254. https://doi.org/10.1175/JPO-D-15-0184.1

Walczowski, W. (2013). Frontal structures in the West Spitsbergen Current margins. *Ocean Science*, *9*(6), 957. https://doi.org/10.5194/os-9-957-2013–975